

The Landscape of Particle Production: Results from PHOBOS

Peter Steinberg¹ for the PHOBOS Collaboration

B B Back², M D Baker¹, M Ballintijn³, D S Barton¹, B Becker¹, R R Betts⁴, A A Bickley⁵, R Bindel⁵, A Budzanowski⁶, W Busza³, A Carroll¹, M P Decowski³, E García⁴, T Gburek⁶, N George^{1,2}, K Gulbrandsen³, S Gushue¹, C Halliwell⁴, J Hamblen⁷, A S Harrington⁷, G A Heintzelman¹, C Henderson³, D J Hofman⁴, R S Hollis⁴, R Hołyński⁶, B Holzman¹, A Iordanova⁴, E Johnson⁷, J L Kane³, J Katzy^{3,4}, N Khan⁷, W Kucewicz⁴, P Kulinich³, C M Kuo⁸, J W Lee³, W T Lin⁸, S Manly⁷, D McLeod⁴, A C Mignerey⁵, R Nouicer^{1,4}, A Olszewski⁶, R Pak¹, I C Park⁷, H Pernegger³, C Reed³, L P Remsberg¹, M Reuter⁴, C Roland³, G Roland³, L Rosenberg³, J Sagerer⁴, P Sarin³, P Sawicki⁶, I Sedykh¹, W Skulski⁷, C E Smith⁴, G S F Stephans³, A Sukhanov¹, J -L Tang⁸, M B Tonjes⁵, A Trzupek⁶, C Vale³, G J van Nieuwenhuizen³, R Verdier³, G I Veres³, F L H Wolfs⁷, B Wosiek⁶, K Woźniak⁶, A H Wuosmaa², B Wysłouch³ and J Zhang³

¹ Brookhaven National Laboratory, Upton, NY 11973-5000, USA

² Argonne National Laboratory, Argonne, IL 60439-4843, USA

³ Massachusetts Institute of Technology, Cambridge, MA 02139-4307, USA

⁴ University of Illinois at Chicago, Chicago, IL 60607-7059, USA

⁵ University of Maryland, College Park, MD 20742, USA

⁶ Institute of Nuclear Physics, Kraków, Poland

⁷ University of Rochester, Rochester, NY 14627, USA

⁸ National Central University, Chung-Li, Taiwan

Abstract. Recent results from the PHOBOS experiment at RHIC are presented, both from Au+Au collisions from the 2001 run and p+p and d+Au collisions from 2003. The centrality dependence of the total charged particle multiplicity in p+p and d+Au show features, such as N_{part} -scaling and limiting fragmentation, similar to $p+A$ collisions at lower energies. Multiparticle physics in Au+Au is found to be local in (pseudo)rapidity, both when observed by HBT correlations and by forward-backward pseudorapidity correlations. The shape of elliptic flow in Au+Au, measured over the full range of pseudorapidity, appears to have a very weak centrality dependence. Identified particle ratios in d+Au reactions show little difference between the shape of proton and anti-proton spectra, while the absolute yields show an approximate m_T scaling. Finally, results on R_{dAu} as a function of pseudorapidity, show that this ratio decreases monotonically with η , even between $0.2 < \eta < 1.4$.

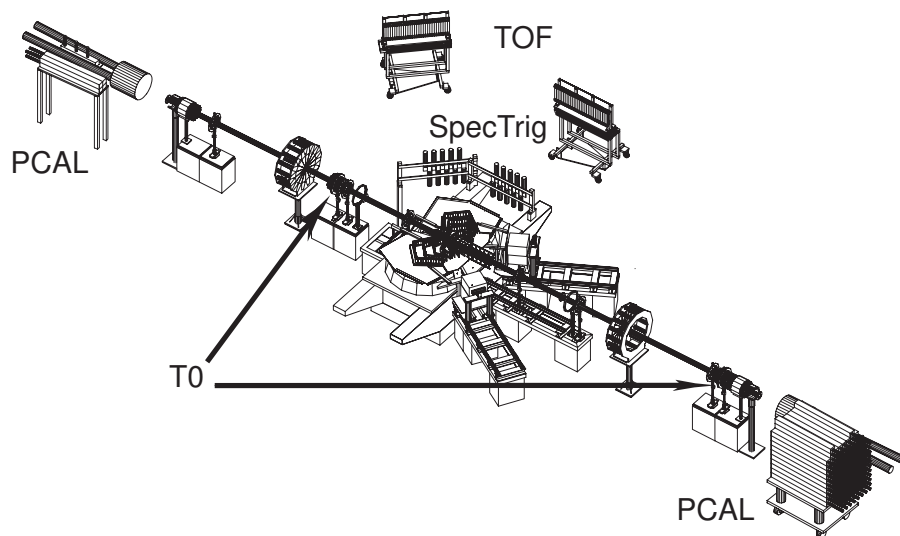


Figure 1. The PHOBOS detector configuration for the 2003 d+Au run.

1. Introduction

The PHOBOS detector at RHIC was designed to offer an overview of particle production in the collisions of a variety of systems (p+p, d+Au, Au+Au) over a wide range of control parameters: beam energy, pseudorapidity, and centrality.

The PHOBOS apparatus was upgraded substantially for the 2003 d+Au RHIC run. Two calorimeters (PCAL) were added to provide information on spectator protons from the d and Au projectiles. Another major upgrade involved the PHOBOS particle-identification system. The two time-of-flight (TOF) walls were moved back from their design position to improve the mass resolution. Time resolution was improved by the addition of two sets of 10 Cerenkov timing start counters (T0). Most importantly, two small hodoscopes were added just behind the PHOBOS spectrometer to provide the means to trigger on high-momentum particles which also hit the TOF walls. This spectrometer trigger (SpecTrig) was installed to enrich the sample of identified particles at high transverse momentum ($p_T = 3 - 4$ GeV/c).

2. Charged-Particle Multiplicity

In 2003, PHOBOS took data at $\sqrt{s_{NN}} = 200$ GeV for both p+p and d+Au collisions. Minimum-bias d+Au data has already been released [1]. As with the d+Au data, the p+p data were corrected for trigger bias in an attempt to estimate the pseudorapidity distribution for the total inelastic cross section. Using the signals in the PHOBOS ring detectors ($3 < |\eta| < 5.4$), the d+Au data has been divided into centrality bins, which are shown in Fig. 2. As with Au+Au collisions, both limiting fragmentation relative to lower-energy proton-nucleus data [2, 3], and participant scaling of the total multiplicity [4] are observed, the latter being shown in Fig. 3. These results are somewhat surprising

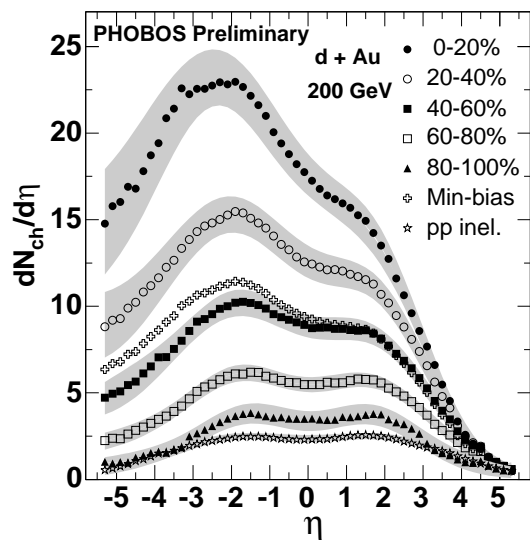


Figure 2. $dN_{ch}/d\eta$ for centrality bins in p+p and d+Au collisions. Bands are 90% C.L. systematic errors. Error bars on min-bias data are suppressed for clarity.

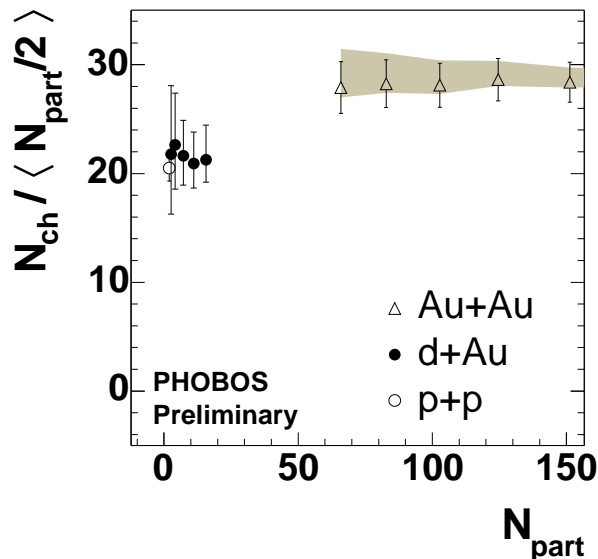


Figure 3. N_{ch}^{d+Au} (integrated over 4π) divided by $\langle N_{part}/2 \rangle$ vs. N_{part} . Error bars are 90% C.L. while the grey band expresses the systematic error on N_{part} in Au+Au.

since different dynamical effects could be expected to dominate in the deuteron and gold hemispheres, such as energy stopping and secondary cascading. The robustness of the N_{part} scaling perhaps suggests some sort of long-range correlation among the produced particles. The different constant of proportionality between the p+p/d+Au data and the Au+Au data also suggests a fundamental difference between the two, once moderate centralities are reached in Au+Au. These results, along with the detailed energy dependence of pseudorapidity distributions in p+A and d+A, are discussed in more detail in Ref. [5].

3. Directed and Elliptic Flow in Au+Au

PHOBOS results on v_2 as a function of pseudorapidity have been shown previously for data integrated over all available centralities [6, 7]. Preliminary results have extended this measurement by a division of the data into three centrality bins, shown in Fig. 4. These results show that the shape is manifestly not boost invariant over all η in peripheral collisions (although one must not ignore kinematic effects near midrapidity, as pointed out by Kolb [8]). Moreover, the shape does not change dramatically as a function of centrality, apart from an overall scale factor.

New at QM2004 are results on v_1 , the first harmonic of the azimuthal angular distribution, as a function of pseudorapidity and beam energy. A simple picture, which considers the effect of the net baryons, would suggest that v_1 should develop opposite

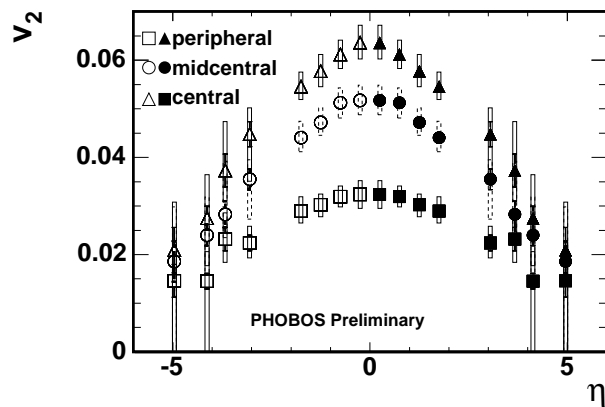


Figure 4. v_2 for 3 centrality bins in 200 GeV Au+Au collisions. Statistical errors are shown as bars. 90% C.L. systematic errors are indicated by boxes.

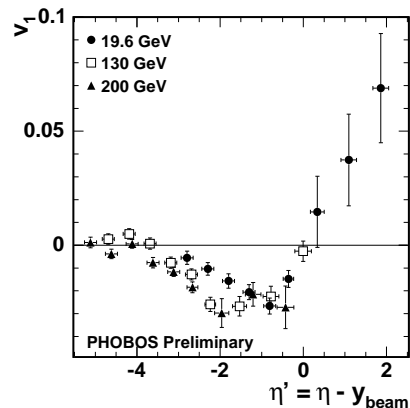


Figure 5. v_1 as a function of η' for Au+Au collisions at three energies. Statistical errors are shown as bars. 90% C.L. systematic errors are suppressed in this figure.

signs for baryons and mesons, with the baryons defined to have a positive directed flow signal near projectile rapidities. Our results on v_1 show a striking energy dependence, which leads to a large range in η with $v_1 \sim 0$ for the higher energies and then a small but systematic negative v_1 that is approximately independent of energy when viewed relative to beam rapidity, shown in Fig. 5. This may be apparently another manifestation of “limiting fragmentation”, already seen in the pseudorapidity distributions of charged particles [9]. Studies such as these should be useful in understanding the global dynamics of Au+Au collisions. These results, along with comparisons to other experimental data, are explained in more detail in Ref. [10].

4. Forward Multiparticle Physics

Another approach to understanding the role of correlations in rapidity space is the use of multi-particle correlation measures like two-particle HBT correlations and forward-backward correlations.

PHOBOS has performed the first measurement of the rapidity dependence of HBT correlations at RHIC. Using the YKP (Yano-Koonin-Podgoretskii) parametrization, we have also been able to correlate the rapidity of the local source as a function of the average rapidities of the two particles. Shown in Fig. 6, one sees that these two rapidities are tightly correlated, suggesting that particles produced at a certain rapidity were produced by a source moving collectively at the same rapidity. This result is similar that found by the NA49 experiment at the SPS. These results are explained in more

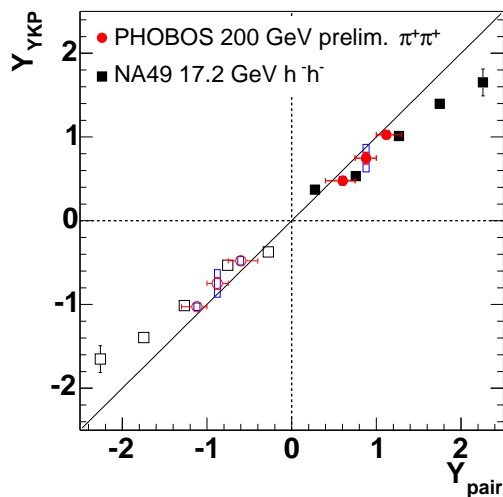


Figure 6. Correlation of the YKP source rapidity with the average rapidity of the pion pair.

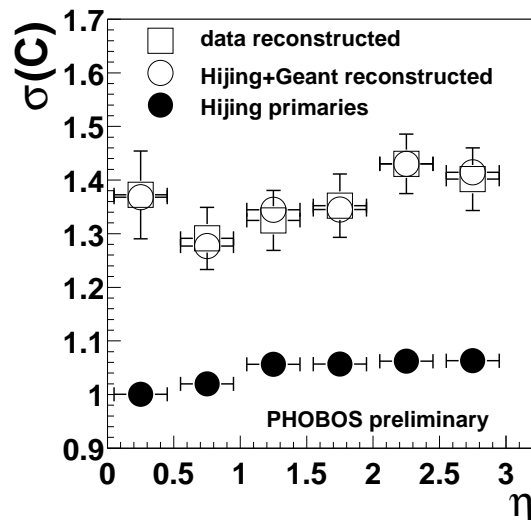


Figure 7. Forward backward correlation measure $\sigma(C)$ vs. η for a bin width of $\Delta\eta = 0.5$.

detail in Ref. [11].

Another indication that multiparticle correlations reflect physics local in rapidity comes from the measurement of forward-backward correlations. One would expect a strong correlation between particles produced in rapidity bins in opposite hemispheres, simply from the fact that particle production is controlled by the number of participants. The quantitative analysis of relative fluctuations can be used to assess the level of short range correlations, which should lead to a non-binomial distribution of multiplicities between two identical bins in the forward (P) and backward (N) directions. By analyzing the variance of a variable $C = (P - N)/\sqrt{P + N}$, $\sigma(C)$, as a function of the total multiplicity $P + N$, compared to a detailed Monte Carlo simulation of our apparatus, we can study non-binomial contributions to the fluctuations. In Fig. 7, we show data on $\sigma(C)$ for a bin width $\Delta\eta = 0.5$ vs. η as open squares. Results from HIJING events are shown for primary charged particles (closed circles) and full simulations (open circles). The deviations of $\sigma(C)$ for the primary charged particles from unity indicate that short-range correlations exist with a mild pseudorapidity dependence for $\eta > 1$. The agreement of the data with the fully-simulated HIJING suggests similar correlations are present in our data set. These results are shown for a different values of $\Delta\eta$ and discussed in detail in Ref. [12].

5. Identified Particle Spectra

One of the major upgrades to the PHOBOS detector in 2003 was the rearrangement of the TOF walls and the addition of a trigger to increase our statistics of events with a

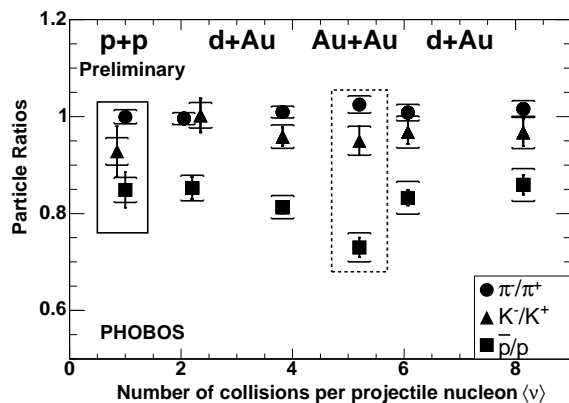


Figure 8. Identified particle ratios in 200 GeV p+p, d+Au, and Au+Au collisions as a function of ν . Statistical errors are shown as bars. 90% C.L. systematic errors are indicated by brackets.

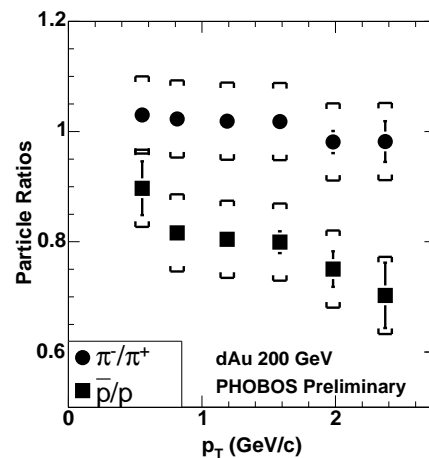


Figure 9. π^-/π^+ and \bar{p}/p ratios vs. p_T in 200 GeV d+Au collisions. Statistical errors are shown as bars. 90% C.L. systematic errors are indicated by brackets.

high-momentum track in the spectrometer. With the enriched data set, we were able to make several new measurements of identified particles at high p_T in d+Au collisions. These results are explained in more detail in Ref. [13].

Ratios of identified particles and anti-particles are a tool to study baryon transport. Various models predict a substantial transport of the initial baryon number of the deuteron all the way to mid-rapidity, leading to a progressive decrease in the \bar{p}/p ratio as a function of the number of collisions of each deuteron participant (characterized by ν) [14]. Our results for this ratio using dE/dx PID, shown in Fig. 8, show surprisingly little centrality dependence for particle momenta below 1 GeV/c and essentially the same result is found in p+p and d+Au. Using the TOF to extend our particle identification from 1.75 GeV/c to 3 GeV/c, this ratio shows a similarly weak centrality dependence. Moreover, this ratio is also weakly dependent on p_T , as seen in Fig. 9. This suggests that proton and anti-proton spectra are similar, except for a difference in overall yield.

The increased statistics in the spectrometer has enabled PHOBOS to measure spectra of identified pions, kaons, and protons of both charge signs up to 3.5 GeV. The presence of a ‘‘Cronin effect’’ in d+Au collisions at RHIC energies has raised the question of whether any particular species is responsible for this effect. We have found that the relative contributions to the inclusive spectra vary substantially with p_T , especially the growing fraction of protons and anti-protons, as shown by the invariant yields plotted vs. p_T in Fig. 10. However, when the yields are shown as a function of m_T , the relative contributions appear to have little m_T -dependence. In other words, an apparent m_T

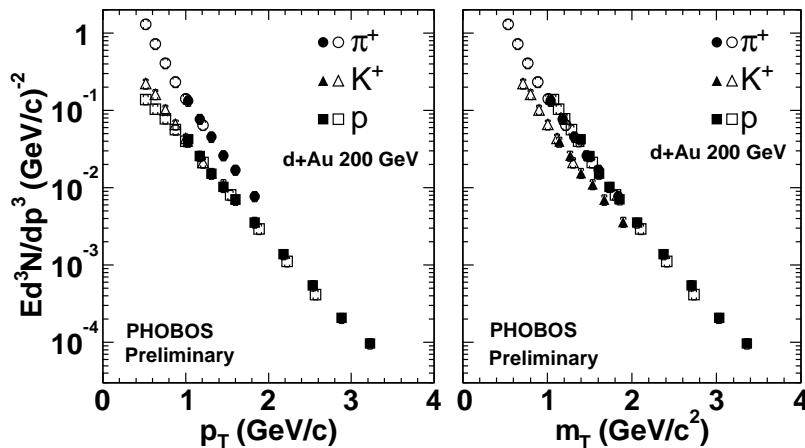


Figure 10. Absolute yields of positively-charged identified particles in 200 GeV d+Au collisions, shown as a function of p_T (left) and m_T (right). The open and closed symbols represent two different bending directions. The data are not corrected for contributions from weak decays. Statistical errors are shown as bars. 90% C.L. systematic errors are indicated by brackets.

scaling is evident in the $d + Au$ data. This is also seen in $p + p$ data, but is dramatically violated at low momentum in Au+Au [15].

6. Inclusive Spectra vs. Pseudorapidity

One of the more striking results from the 2003 data is the observation of a significant η dependence in the modification of $d + Au$ spectra relative to $p + p$ data [16, 17]. This has been interpreted as an indication of the onset of parton saturation [18] in the forward region. To address this topic, PHOBOS has repeated its measurement of R_{dAu} , originally integrated over our full acceptance ($0.2 < \eta < 1.4$) [17], but now in three bins ($0.2 < \eta < 0.6$, $0.6 < \eta < 1.0$, and $1.0 < \eta < 1.4$). Even within the acceptance of the PHOBOS spectrometer, $\Delta\eta = 1.2$ units, a dramatic drop in this ratio is seen as a function of η . When compared with other results from RHIC in Fig. 11, it is found that the suppression seen at forward rapidities is a continuation of a trend started already at midrapidity. Measurements in the backward hemisphere by PHENIX show a clear enhancement of pion production with $1 < p_T < 3$ GeV/c [19], suggesting that this is not an effect that “turns on” in the forward region, but rather part of a difference between $p + p$ and $d + Au$ data that extends over a large range in η .

7. Conclusions

Recent p+p, d+Au, and Au+Au results at 200 GeV from the PHOBOS experiment at RHIC have been presented. The systematic measurements shown here should serve as a useful baseline for understanding the differences between heavy ion collisions and more elementary systems.

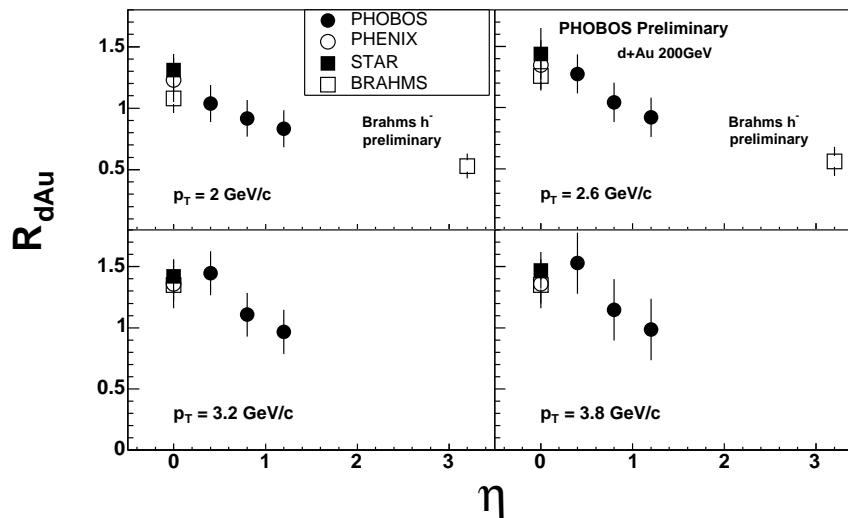


Figure 11. R_{dAu} at fixed values of p_T shown as a function of η , compared with results from other RHIC experiments. Error bars are statistical only.

Acknowledgments

This work was partially supported by U.S. DOE grants DE-AC02-98CH10886, DE-FG02-93ER40802, DE-FC02-94ER40818, DE-FG02-94ER40865, DE-FG02-99ER41099, and W-31-109-ENG-38, by U.S. NSF grants 9603486, 0072204, and 0245011, by Polish KBN grant 2-P03B-10323, and by NSC of Taiwan under contract NSC 89-2112-M-008-024.

References

- [1] B. B. Back *et al*, arXiv:nucl-ex/0311009.
- [2] W. Busza, *Acta Phys. Polon. B* **8**, 333 (1977).
- [3] J. E. Elias *et al*, *Phys. Rev. D* **22**, 13 (1980).
- [4] B. B. Back *et al*, arXiv:nucl-ex/0301017.
- [5] R. Nouicer *et al*, these proceedings.
- [6] B. B. Back *et al*, *Phys. Rev. Lett.* **89**, 222301 (2002).
- [7] S. Manly *et al*, *Nucl. Phys. A* **715**, 611 (2003).
- [8] P. F. Kolb, *Acta Phys. Hung. New Ser. Heavy Ion Phys.* **15**, 279 (2002).
- [9] B. B. Back *et al*, *Phys. Rev. Lett.* **91**, 052303 (2003).
- [10] M. Belt Tonjes *et al*, these proceedings.
- [11] B. Holzman *et al*, these proceedings.
- [12] K. Wozniak *et al*, these proceedings.
- [13] G. I. Veres *et al*, these proceedings.
- [14] B. B. Back *et al*, arXiv:nucl-ex/0309013.
- [15] B. B. Back *et al*, arXiv:nucl-ex/0401006.
- [16] I. Arsene *et al*, arXiv:nucl-ex/0403005.
- [17] B. B. Back *et al*, *Phys. Rev. Lett.* **91**, 072302 (2003).
- [18] J. Jalilian-Marian, these proceedings.
- [19] M.-X. Liu *et al*, these proceedings.